Lucero, C., Brookshire, G., Sava-Segal, C. Bottini, R., Goldin-Meadow, S., Vogel, E., & Casasanto, D. (2020). Unconscious number discrimination in the human visual system. *Cerebral Cortex.* DOI:10.1093/cercor/bhaa155

Unconscious number discrimination in the human visual system

Ché Lucero, Geoffrey Brookshire, Clara Sava-Segal

University of Chicago

Roberto Bottini

University of Trento

Susan Goldin-Meadow, Edward K. Vogel, and Daniel Casasanto

University of Chicago

Author Note

Ché Lucero, Geoffrey Brookshire, Clara Sava-Segal, Susan Goldin-Meadow, Edward K. Vogel, and Daniel Casasanto, Department of Psychology, University of Chicago.

Roberto Bottini, Center for Mind/Brain Sciences (CiMEC), University of Trento, Italy.

Ché Lucero and Daniel Casasanto are now at the Department of Human Development, Cornell University. Geoffrey Brookshire is now at the School of Psychology, University of Birmingham. Clara Sava-Segal is now at the Department of Neurology & Neurological Sciences, Stanford University School of Medicine.

Abstract

How do humans compute approximate number? According to one influential theory, approximate number representations arise in the intraparietal sulcus and are amodal, meaning that they arise independent of any sensory modality. Alternatively, approximate number may be computed initially within sensory systems. Here we tested for sensitivity to approximate number in the visual system using steady state visual evoked potentials (SSVEPs). We recorded electroencephalography (EEG) from humans while they viewed dotclouds presented at 30 Hz, which alternated in numerosity (ranging from 10 to 20 dots) at 15 Hz. At this rate, each dotcloud backward masked the previous dotcloud, disrupting top-down feedback to visual cortex and preventing conscious awareness of the dotclouds' numerosities. Spectral amplitude at 15 Hz measured over the occipital lobe (Oz) correlated positively with the numerical ratio of the stimuli, even when non-numerical stimulus attributes were controlled, indicating that subjects' visual systems were differentiating dotclouds on the basis of their numerical ratios. Crucially, subjects were unable to discriminate the numerosities of the dotclouds consciously, indicating the backward masking of the stimuli disrupted reentrant feedback to visual cortex. Approximate number appears to be computed within the visual system, independently of higher-order areas such as the intraparietal sulcus.

Keywords: approximate number system, consciousness, occipital, SSVEP, vision

Introduction

Humans have a remarkable capacity for working with numbers. Symbolic mathematical ability is hard earned, requiring explicit instruction and prolonged practice. Starting early in life, however, humans can rapidly assess approximate number with no training, an ability many researchers attribute to an *approximate number system* (ANS; Dehaene et al. 1998). The intraparietal sulcus has been implicated as an important area supporting number processing, with many studies suggesting the intraparietal sulcus as the site where number representations arise. An alternative proposal suggests that the visual system may calculate number directly (e.g., Burr and Ross 2008). Experiments testing this proposal have localized number-sensitive signals to the occipital cortex but leave open the possibility that a higher-order cortical area like the intraparietal sulcus computes number and feeds this numerical information back to the visual system. In this study, we observe number-sensitive signals in the visual system under experimental conditions that disrupt reentrant feedback to the occipital cortex. Thus, we conclude that the visual system can compute number directly.

The Intraparietal Sulcus as the Locus of Number Representations

According to some researchers, the intraparietal sulcus is where number representations arise (Dehaene et al. 1999; Nieder 2016; Nieder and Miller 2004; Pinel et al. 2001; Zorzi et al. 2002). This suggestion is consistent with the observation that intraparietal sulcus responds to numerosities regardless of their sensory modality (Dehaene et al. 1998; Dehaene et al. 2003; Eger et al. 2003) and that adaptation to number has been found across sensory modalities (Arrighi et al. 2014). In light of this apparent modality-independence, the intraparietal sulcus is

believed to be "the first cortical hub to extract quantitative information" from stimuli (Nieder 2016, pg. 369).

The evidence that the intraparietal sulcus is involved in approximate number processing is strong and varied, including studies using positron emission tomography (e.g. Dehaene et al. 1996), functional magnetic resonance imaging (Naccache and Dehaene 2001; Piazza et al. 2007), transcranial magnetic stimulation (Andres et al. 2011; Cappelletti et al. 2007; Göbel et al. 2006), and clinical populations with brain lesions (Cipolotti et al. 1991; Dehaene and Cohen 1997). Yet, although it is clear that the intraparietal sulcus is involved in number processing, it is unclear whether this is the site (or the *only* site) where approximate number representations arise.

Is Number Also Computed in the Visual System?

In addition to amodal number representations in the intraparietal sulcus, could number processing also occur within sensory systems? On one proposal, number may be processed as "a primary visual property like color or motion" (Burr and Ross 2008, pg. 1). Initial evidence for this proposal relied on behavioral adaptation effects (Burr and Ross 2008; Ross and Burr 2010). Subsequent neuroimaging studies have localized number-sensitive signals to the visual cortex using fMRI (DeWind et al. 2018, Castaldi et al. 2019, Cavdaroglu and Knops 2019) and EEG (e.g. Park et al. 2015; Fornaciai et al. 2017).

One approach to testing for numerosity processing in the visual system is to evoke Steady State Visual Evoked Potentials (SSVEPs). SSVEPs are "exogenous ERPs...generated in response to a train of stimuli presented at a fixed rate" (Norcia et al. 2015, pg. 1). Typically, stimuli in a train alternate between two values (e.g., a square patch switching between two levels of brightness), and the SSVEP emerges at the frequency of the alternation. The magnitude of the

SSVEP signal increases as the magnitude of difference in the alternating values increases (the SSVEP would be stronger when the stimuli brightness alternated between 1000 and 3000 lux than alternating between 1000 and 1200 lux). SSVEP paradigms have been used for over half a century to probe the visual system (Regan 1989), and the occipital lobe has been identified as the primary source of the SSVEP signal using EEG, MEG, PET, and fMRI (e.g. Andersen et al. 2008; Di Russo et al. 2007; Fawcett et al. 2004; Hillyard et al. 1997; Müller et al. 1997; Sammer et al. 2005; c.f. Thorpe et al. 2007).

The SSVEP paradigm can be adapted to test for a subject's sensitivity to the numerosity of the stimulus by changing the numerical content within a stimulus stream at some fixed interval. If the subject is sensitive to the changes in numerosity, the changes will evoke an SSVEP at that frequency. Researchers have successfully used variants of this approach to record number-sensitive SSVEPs from adults (Guillaume et al. 2018; Park 2018), and children (Libertus et al. 2011; Park 2018).

On the basis of SSVEP and fMRI studies showing number-sensitive signals in the occipital cortex (DeWind et al. 2018; Fornaciai et al. 2017; Park et al. 2015), researchers have claimed that the occipital cortex is calculating numerosity from visual input, suggesting that "visual quantities are perceptually discriminated automatically and rapidly (i.e., at a glance) within the occipital cortex." (Guillaume et al. 2018, pg. 180). These findings have been interpreted as “strong support for the hypothesis that number is rapidly and directly encoded early in the visual processing stream." (DeWind et al. 2018, Pg. 76), and as confirmation that "number is encoded rapidly and directly very early in the visual processing stream" (Doricchi et al. 2019, pg. 1).

Can the claim that the visual system computes number be supported by observations of

number-sensitive signals in the occipital cortex? Under a skeptical interpretation, number-related activity in the occipital cortex could result from number computations in classical number areas (e.g. intraparietal sulcus) which feed the resulting numerosity representation back down to occipital cortex. The visual system produces feedforward sweeps from the occipital cortex to higher-order cortical areas, followed by reentrant feedback to the occipital cortex (Dehaene et al. 2006; Lamme and Roelfsema 2000). It is possible to interpret studies showing number sensitive signals in occipital cortex as evidence that number is computed there (DeWind et al. 2018; Doricchi et al. 2019). However, these studies are also consistent with the view that the intraparietal sulcus is where number representations originate (Dehaene et al. 1999; Nieder 2016). Number sensitive activity in occipital cortex could reflect feedback from the intraparietal sulcus, where number was computed, first.

To distinguish these two possibilities and to clarify the first cortical locus of approximate number representation, in the present study we presented visual numerosity stimulation while disrupting reentrant feedback to the occipital cortex.

The Present Study

Here we report an SSVEP experiment testing whether occipital cortex responds to the numerosity of visual stimuli under conditions that disrupt feedback from higher-order cortical areas to the occipital cortex. We designed trains of stimuli to take advantage of a known property of SSVEPs: The magnitude of the evoked response increases with the magnitude of the difference between the alternating stimuli. Therefore, we varied the numerical ratio of the alternating dotclouds between trains of stimuli in order to probe subjects' visual sensitivity to different numerosities. If the occipital cortex, per se, is sensitive to the numerical content of the

dotclouds, then the strength of the SSVEP should increase as the dotcloud ratios increase. Observed SSVEPs should be weak for close ratios that are difficult for humans to discriminate reliably (e.g., 10 : 11 dots) and should increase asymptotically, plateauing at large ratios that are equally easy to discriminate (as is typically found for behavioral measures of approximate number discrimination; e.g., Libertus et al. 2012).

To ensure that the observed SSVEPs index sensitivity to the numerosity of the stimuli, as opposed to sensitivity to other visual attributes, we constructed the stimuli according to a method developed by DeWind, Adams, Platt, and Brannon (DeWind et al. 2015). This method allows the numerical content of the stimuli to be partially orthogonalized with respect to the non-numerical content, and for non-numerical magnitudes to be controlled.

Unlike previous tests of number processing in occipital cortex (including previous SSVEP tasks, e.g., Park 2018), here we used backward masking to disrupt reentrant feedback in order to test for number computations within occipital cortex, per se. Visual input is initially processed in a feedforward sweep from lower- to higher-order areas. Although visual areas respond selectively to complex stimuli during the feedforward sweep (e.g., faces; Oram and Perret 1992), feedforward processing is not sufficient for viewers to identify the stimuli consciously (Lamme 2006; Lamme and Roelfsema 2000). Conscious awareness appears to depend on subsequent reentrant feedback involving fronto-parietal areas feeding back to lower-level visual areas (Dehaene et al. 2006; Di Lollo et al. 2000; Dux et al. 2010; Lamme 2003; Lamme and Roelfsema 2000).

Backward-masking a target stimulus by rapidly presenting a new stimulus reduces or eliminates awareness of the first stimulus. The masking stimulus elicits a new cascade of feedforward activity, changing the state of the visual cortex as it processes the new stimulus.

This feedforward activity disrupts the integration of reentrant feedback from higher-order areas that is necessary for conscious visual awareness (Fahrenfort et al. 2007).

To achieve backward masking, we present dotcloud stimuli with 33 ms between stimulus onsets. Each dotcloud acts as a backward mask for the previous stimulus. If subjects are unable to report on the numerical contents of the stimulus, this would indicate that backward-masking disrupted the reentrant processing that leads to conscious awareness of approximate number. If the occipital cortex is insensitive to stimulus numerosity under these conditions, this result would support the hypothesis that numerosity is first calculated in the intraparietal sulcus and fed back down to the occipital cortex. Alternatively, if a number-sensitive SSVEP is observed during unconscious processing of the backward-masked dotcloud stimuli, this result would support the hypothesis that approximate number representations can originate within the occipital cortex.

Materials and Methods

Participants Twenty-one adults from the University of Chicago community participated for cash compensation. Subjects had normal or corrected-to-normal vision. All subjects provided informed consent in writing.

Dotcloud Stimuli Stimuli consisted of eleven sets of dotclouds. Each stimulus set contained 288 unique dotclouds. In a given set, half of the dotclouds had ten dots per cloud, and half had a single comparison number of dots. The eleven comparison quantities ranged from from ten dots to twenty dots. All dots within a given dotcloud were the same size. Dotclouds were constructed so that the number comparison increased across sets (i.e. 10:10, 10:11, 10:12, up to 10:20). Size (total surface area, individual dot surface area) and spacing (convex hull, sparsity) attributes

were selected so that they varied across sets but did not systematically differ across the range of number comparisons. The stimuli were constructed so that the magnitude of variation within each attribute changed across trials. Importantly, the change in the magnitude of variation across trials differs between numerical and non-numerical attributes (Figs. 2 and 3), peaking in the middle of the range of dotcloud values for non-numerical attributes but increasing linearly for number, thus allowing statistical separation of their effects.

Design and Procedure Subjects completed two tasks across two hours. The first task ("fast presentation of dotclouds") involved passively viewing series of dotcloud stimuli flashing at 30 Hz presented with PsychoPy2 v1.84.0 (Peirce 2007) while EEG was recorded. Each dotcloud was on screen for 16.7 ms, with a 16.7 ms ISI between dotclouds. Each trial contained 9.6 seconds of dotcloud stimulation, after which subjects were asked to make a numerosity judgment: “Did all the dotclouds have the SAME quantity, or did some have a DIFFERENT quantity?” The subjects responded verbally, and the experiment recorded their answer with a keystroke (“s” or “d”). See Figure 1 for the trial structure. A block consisted of eleven trials. Each trial presented one of the eleven unique sets of dotcloud stimuli. Subjects completed as many blocks as possible in the first task for about 80 minutes. The completed number of blocks ranged from 15 to 24 blocks (165 to 264 trials). We then stopped recording EEG and they began the second task ("slow dotcloud presentation"). In the second task, subjects were presented dotclouds in pairs. After each pair of dotclouds was presented, subjects were asked to make a numerosity judgment: “Did both dotclouds have the SAME quantity, or did they have DIFFERENT quantities?” Subjects recorded their response with a keystroke (“s” or “d”). Dotclouds were randomly chosen as an adjacent pair from one of the eleven unique sets of stimuli used during fast dotcloud presentation. Dotcloud stimuli were presented serially to the

subject. Each dotcloud remained on-screen for 200 ms, with a 100 ms inter-stimulus interval between presentation of the first and second dotcloud. A block consisted of eleven trials. Each trial presented one pair of dotclouds and contained a unique number comparison (e.g. 10:17). Subjects completed as many blocks as possible for about 10 minutes, and then the task was ended. During both tasks, the background was grey (#7F7F7F). All dots were orange (#FFA500). All on-screen text was white (#FFFFFF), as was a fixation cross that appeared 2000 ms before dotcloud stimulation began and remained on screen until the end of the trial. Subjects sat in a chair with their head approximately twenty-four inches away from the screen. At the start of all trials in the both tasks, the screen went grey and the fixation-cross appeared. After a two second delay, the dotcloud stimulation began.

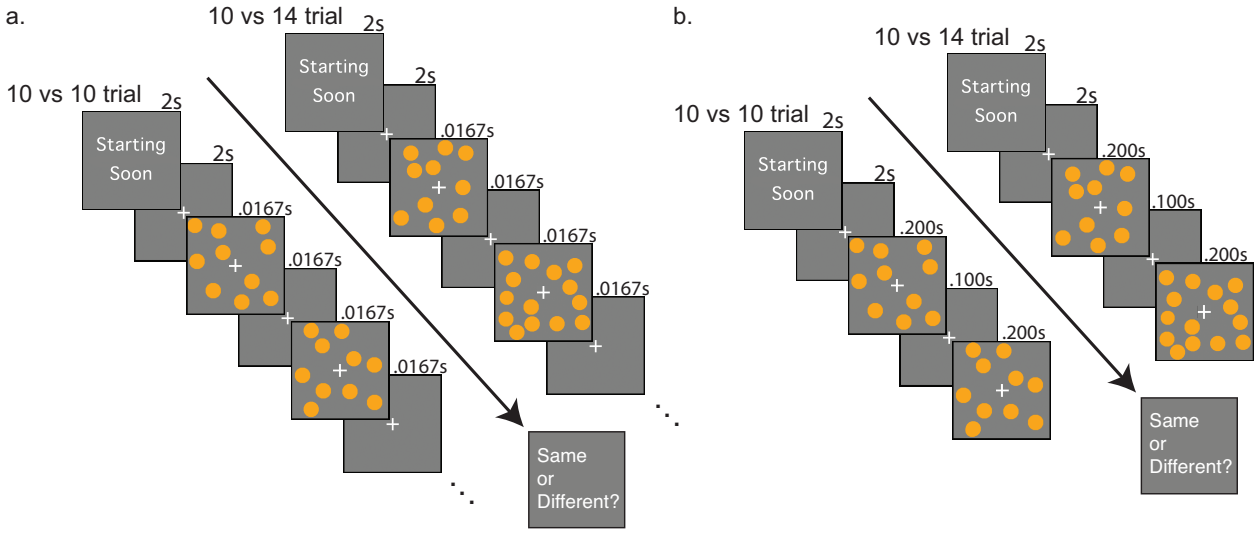

Figure 1. Trial structure of the two tasks. (a) During fast dotcloud presentation, we recorded EEG while subjects watched dotclouds flashing on screen at 30 Hz. On each trial after 9.6 seconds of dotcloud stimulation, subjects judged whether all of the dotclouds had the same number of dots, or if some differed. (b) During slow dotcloud presentation, two dotclouds were

presented and then subjects judged whether they differed in number. Each dotcloud was presented for 200 ms, with a 100 ms inter-stimulus interval.

EEG Acquisition We collected EEG data using a whole-head 128-channel HydroCell Geodesic Sensor Net (Electrical Geodesics Inc., Eugene, OR), bandpass filtered from 0.1 to 100 Hz, and digitized at a rate of 250 Hz (Net Amps 200 TM, Electrical Geodesics, Inc.). Individual electrodes were adjusted until impedances were below 50 kΩ before recording. About every 10 minutes during breaks in-between blocks of stimuli, we checked for and corrected any electrode impedances that had risen above 50 kΩ. Using Netstation software, we exported recordings into a MATLAB-readable format (.raw). Subsequent analyses in MATLAB and R used the Fieldtrip toolbox (Oostenveld et al. 2011) and custom software.

Analysis of SSVEPs Our analysis of the EEG signal recorded during fast presentation of dot clouds used the 15 Hz spectral amplitude of dotcloud stimuli attributes to predict the change in the strength of the observed 15 Hz SSVEP. We analyzed the 15 Hz frequency because the number of dots per dotcloud alternated at 15 Hz during the task. Dotcloud stimulation was being presented at 30 Hz. For a 15 Hz SSVEP to arise, the subject must be differentiating the dotclouds using some attribute of the stimulus that alternated at 15 Hz. We focused our SSVEP analyses on the Oz sensor. Oz is a typical choice for measuring SSVEPs because it is located centrally over occipital (visual) cortex. We calculated a signal-to-noise ratio (SNR) of the 15 Hz SSVEP to create a measure that was comparable across subjects and trials. We converted the recorded EEG signal on each 9.6 second trial (2400 samples) into the frequency domain with a Hanning window fast Fourier transform. We then divided the amplitude in the 15 Hz bin by the average amplitude in the 10 frequency bins adjacent on either side, yielding the SNR measure (following

Rossion et al. 2012; Srinivasan et al. 1999). We excluded the two bins closest to 15 Hz in order to reduce roll-off contamination, calculating the noise as the average amplitude in the frequency bins 13.85 Hz to 14.79 Hz, and 15.20 Hz to 16.14 Hz. The frequency bins were spaced about 0.1 Hz apart. The SNR measure normalizes the signal, protecting against electrode recording idiosyncrasies (e.g. impedance drift) across subjects and blocks. We calculated the coefficient of variation for the raw 15 Hz signal and for the 15 Hz SNR within each trial type (e.g. 10:17). The mean coefficient of variation was five times greater for the raw signal than it was for the SNR (two-sided paired $t(20) = 4.42$, $p = .001$), indicating that the SNR was a more reliable measure of the SSVEP across subjects and trials.

Analysis of Stimulus Attributes We performed a spectral analysis of the stimuli to extract the 15 Hz oscillations of seven dotcloud stimuli attributes within each stimulus set. Using a hanning-window Fourier transform, we calculated the 15 Hz amplitude for Number, Total Surface Area, Individual Dot Size, Convex Hull, and Sparsity.[1] We included two amalgam measures in the spectral analysis, Size and Spacing, which respectively capture the size and spacing aspects of the dotcloud stimuli that are independent of numerosity (see DeWind et al. 2015 for details). Size is defined as $\log_2(\text{Size}) = \log_2(\text{Total Surface Area}) + \log_2(\text{Individual Dot Size})$, and Spacing as $\log_2(\text{Spacing}) = \log_2(\text{Convex hull}) + \log_2(\text{Sparsity})$. We also calculated the 15 Hz amplitude of stimulus contrast energy (Kukkonen et al. 1993, Parish and Sperling 1991).

[1] Convex hull and field area are two closely-related features that capture an aspect of dotcloud spacing. Convex hull is defined as the smallest enclosing polygon without concavity that encompasses all of the dots in a cloud. Field area is defined as the smallest circle that encompasses all of the dots in a cloud. In our stimuli, convex hull and field area were highly correlated ($r = .96$, $p < .001$). In the Results section we report analyses that adopt convex hull as the measure, but we also analyzed the data using field area in place of convex hull. The reported effects of number remain robust no matter whether analyses include field area or convex hull.

Contrast energy is the sum of squared contrast values for all pixels in a stimulus. The occipital cortex, particularly early occipital cortex (Dumoulin et al. 2008), is sensitive to the contrast energy of a stimulus. We calculated contrast energy as $\sum\sum C^2(x,y)$, where the local contrast for an individual pixel $C(x,y)$ is calculated as $(L(x,y) - L_0) / L_0$ with $L(x,y)$ being the luminance of the pixel (taken as its greyscale value) and L_0 being the mean luminance across all pixels in the stimulus.

We created time-series data that simulated how the magnitude of a given stimulus attribute (e.g. total surface area) changed over time during the experiment in a given stimulus set. We created time points from 0 to 9.6 seconds with 3.3 ms spacing (300 Hz sampling). We then created values at each timepoint matching the magnitude of the attribute as displayed to the subject during the experiment. For timepoints coinciding with blank (grey) screens, we entered 0. For timepoints with a dotcloud stimulus on screen, we entered the magnitude of the attribute of interest (e.g. total number of orange pixels for total surface area). We used a Fourier transform to extract the spectral amplitude at 15 Hz for the seven spatial attributes of interest as well as contrast energy within each of the eleven stimulus sets. See Fig. 2 and Fig. 3 for the 15 Hz spectral amplitude of the attributes plotted as a function of the number comparison in that stimulus set.

When preparing the spectral amplitude values of each attribute for charting, we normalized the values for easier visualization. Each attribute had eleven amplitude values; one for each trial type. For each attribute, we normalized the eleven values to fall between 0 and 1, with the largest value set to 1. This operation preserved the ratio between values for a given attribute across trials. Direct comparisons of amplitude between attributes are meaningless with or without normalization. However, normalizing the values to fall in the same range allows

visual comparison of the way each attribute's amplitude changes across trials.

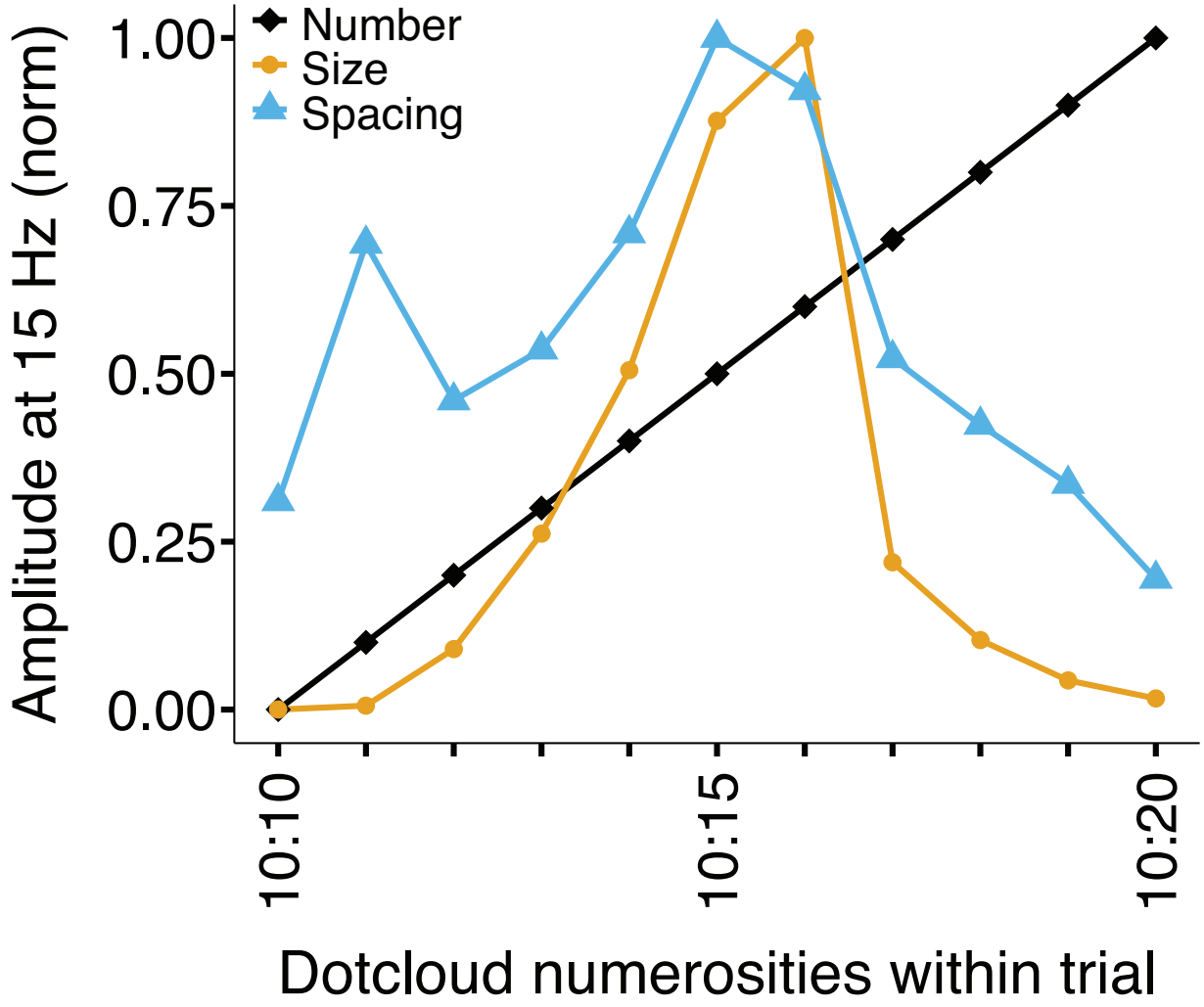

Figure 2. Normalized spectral amplitude for dotcloud attributes number, size, and spacing, plotted as a function of the numerical ratio of dotclouds in each trial. The amplitude value shows how much an attribute changed at 15 Hz during fast dotcloud presentation. The change in amplitude for number across trials dissociates from the changes in amplitude of other dotcloud attributes.

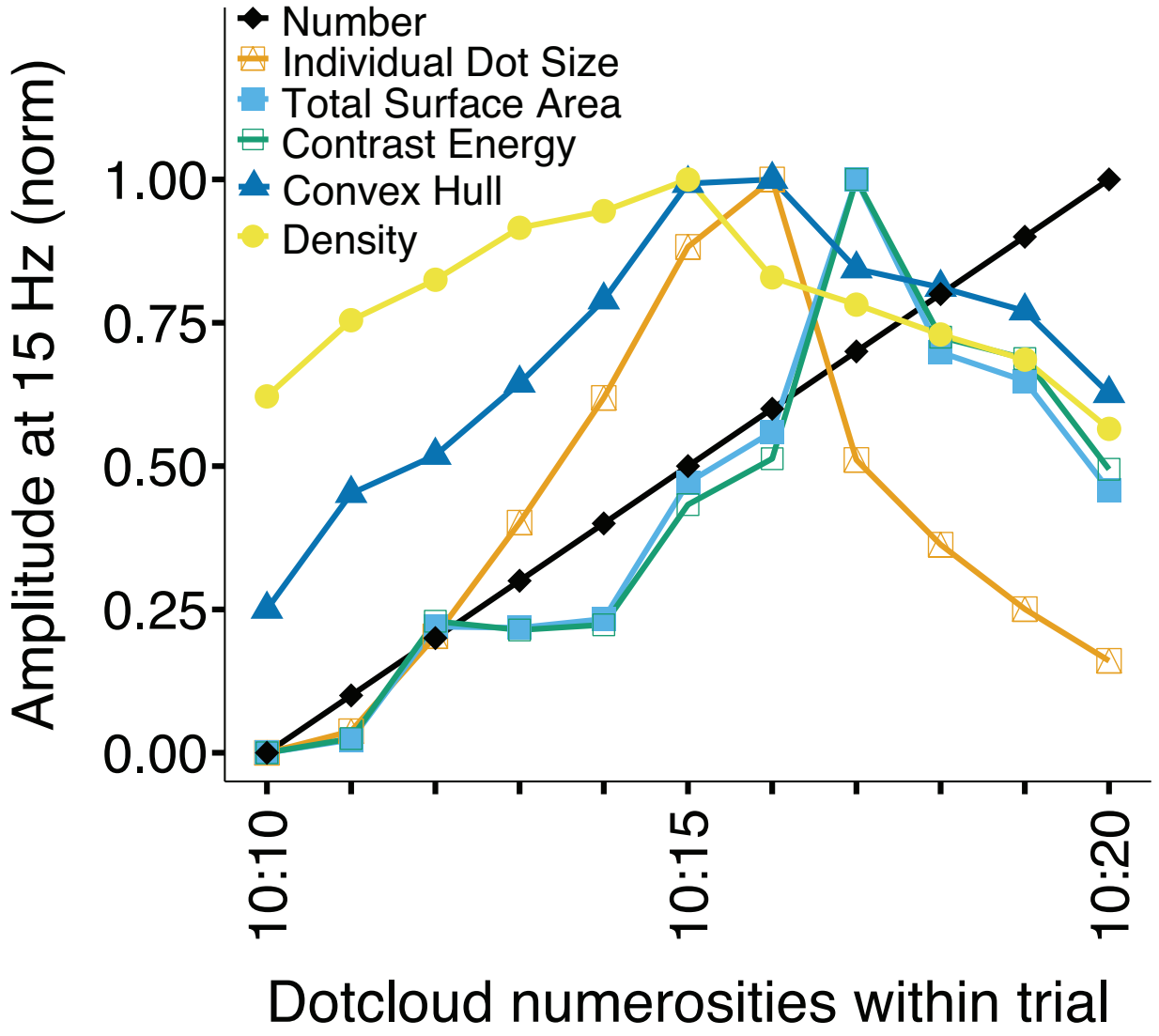

Figure 3. Normalized spectral amplitude for stimulus contrast energy, plus the dotcloud spatial attributes number, individual dot size, total surface area, sparsity (labeled density), and convex hull, plotted as a function of the numerical ratio of dotclouds in each trial. The amplitude value shows how much an attribute changed at 15 Hz during fast dotcloud presentation. The change in amplitude for number across trials dissociates from the changes in amplitude of other dotcloud attributes. Contrast energy (green, unfilled boxes) and total surface area (blue, filled boxes) are almost perfectly correlated.

Regression analyses To model the influence the various stimuli attributes had on the strength of the SSVEP signal, we predicted changes in the SSVEP SNR across trials using the 15 Hz spectral amplitude of the stimulus attributes as regressors. Regression analyses were done using R v3.3.1 (R Core Team 2017) with the lme4 package v1.1-12 (Bates et al. 2015). We modeled subjects as a random effect, and the 15 Hz spectral amplitude of the stimulus attributes as fixed effects. When testing for an effect of interest we used a maximal approach (Barr et al. 2013). We included random by-subject slopes for that effect (e.g. by-subject slopes for number when testing for an effect of number) as well as by-subject intercepts. To test for statistical significance, we used likelihood ratio tests to compare the log likelihood of a full regression model to the log likelihood of a reduced model without the term of interest. This procedure yields degrees of freedom, a chi-square value, and a *p* value. In the EEG data, each data point of observed SNR was labeled with subject, trial number, comparison (e.g. "10 vs. 17"), and 15 Hz amplitude values for each of the eight stimulus attributes. All regression models used the entire dataset with no averaging or exclusions. In the behavioral datasets from our custom experiment scripts (two datasets, one each from the two tasks), we used the numerical ratio of the dotclouds to predict the same (0) or different (1) judgments with logistic regression. The numerical ratio was the comparison dotcloud number (from 10 to 20) divided by the standard dotcloud number (10), and ranged from 1.0 to 2.0 in 0.1 increments. Figures 4 and 5 present SNR calculated on a per-trial basis with scalar averaging; only the amplitudes of Fourier components were used in the calculations. Figures 7 and 8 (see supplementary materials) present versions of the charts with SNR calculated using vector-averaging, which considers phase information along with the

amplitudes.

Results

Fast dotcloud presentation: Were subjects sensitive to number per se?

During fast dotcloud stimulation, changes in number predicted changes in the observed 15 Hz SNR (b = 0.44, $\chi^2(1) = 15.29$, $p < .001$; Fig. 4). Grand averaging of the 15 Hz SSVEP showed it was centered over posterior mid-line sensors (Fig. 5).

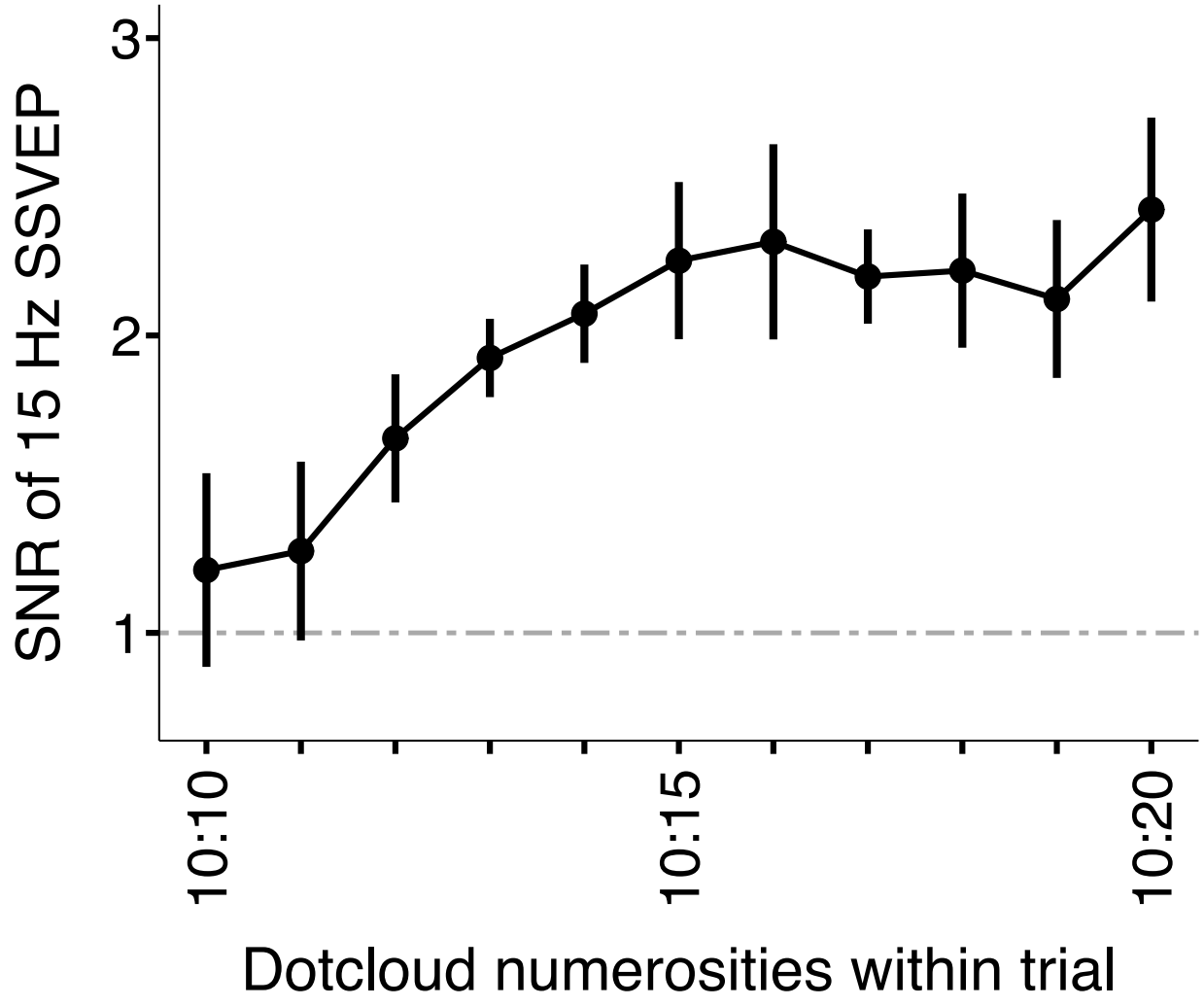

Figure 4. The signal to noise ratio of the 15 Hz SSVEP increases with greater differences in dotcloud numerosity. The dashed line indicates a signal-to-noise ratio of 1. Error bars denote

95% confidence intervals.

Number predicted changes in SNR while controlling for size and spacing related attributes of the dotcloud stimuli: while controlling for total surface area and individual dot size (b = 0.43, $\chi^2(1) = 14.29$, $p < .001$), and while controlling for the amalgam measure Size (b = 0.43, $\chi^2(1) = 14.75$, $p < .001$). Number also predicted SNR while controlling for the spacing-related attributes of convex hull and sparsity (b = 0.44, $\chi^2(1) = 13.94$, $p < .001$), and while controlling for the amalgam measure Spacing (b = 0.48, $\chi^2(1) = 17.17$, $p < .001$). Finally, we controlled for Size, Spacing, and their interaction, finding that number continued to predict changes in the SNR (b = 1.00, $\chi^2(1) = 15.41$, $p < .001$).

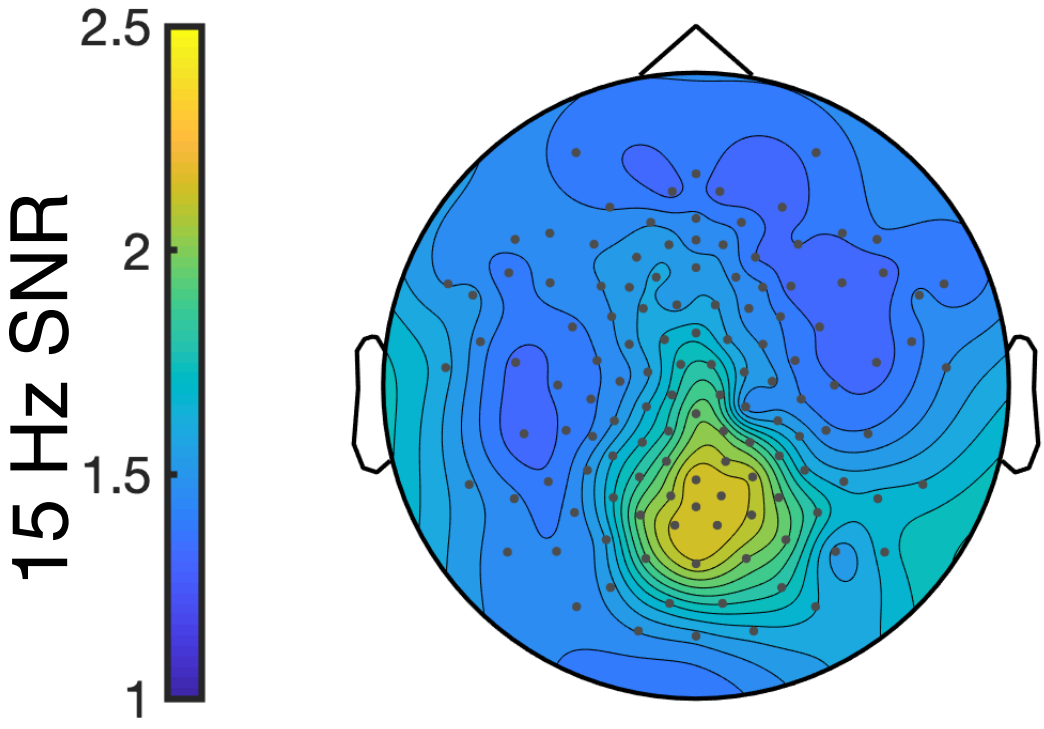

Figure 5. Grand averaged SSVEP signal shows greatest SNR over posterior mid-line sensors.

Contrast energy was almost perfectly correlated with the total surface area of the display (r=.996). Therefore, the results reported above that controlled for the total surface area of the dots suggest that the relationship between the SNR and number cannot be explained by the contrast energy of the stimuli. Furthermore, all of effects of Number reported above remain significant when contrast energy was added to the models (all p's < .01).

Fast dotcloud presentation: Were subjects conscious of the changes in number?

The EEG data during fast dotcloud stimulation shows the subjects were responding to the numerical content of the dotclouds. However, we found that the subjects' explicit numerosity judgments did not depend on the numerical ratio of the dotclouds (OR = 1.20, $\chi^2(1) = 0.71$, p = 0.400; Fig. 6). Despite roughly 90% of their trials containing dotclouds with different numbers of dots, subjects judged all the dotclouds to have the same number of dots about half the time. Although accuracy was poor, there could be a relationship between the EEG signal and judgment behavior. We tested whether subjects were more likely to judge dotclouds as differing in number on trials where they had a higher SNR but did not detect a relationship (OR = 1.019, $\chi^2(1) = 1.61$, p = .204).

Could subjects judge the numerical content when dotclouds were presented slowly?

When presented with the same dotcloud stimuli more slowly (200 ms per dotcloud, 100 ms inter-stimulus interval) in pairs, subjects showed a strong dependence on numerical ratio in their same-or-different judgments (OR = 363.072, $\chi^2(1) = 31.318$, $p < .001$; Fig. 6).

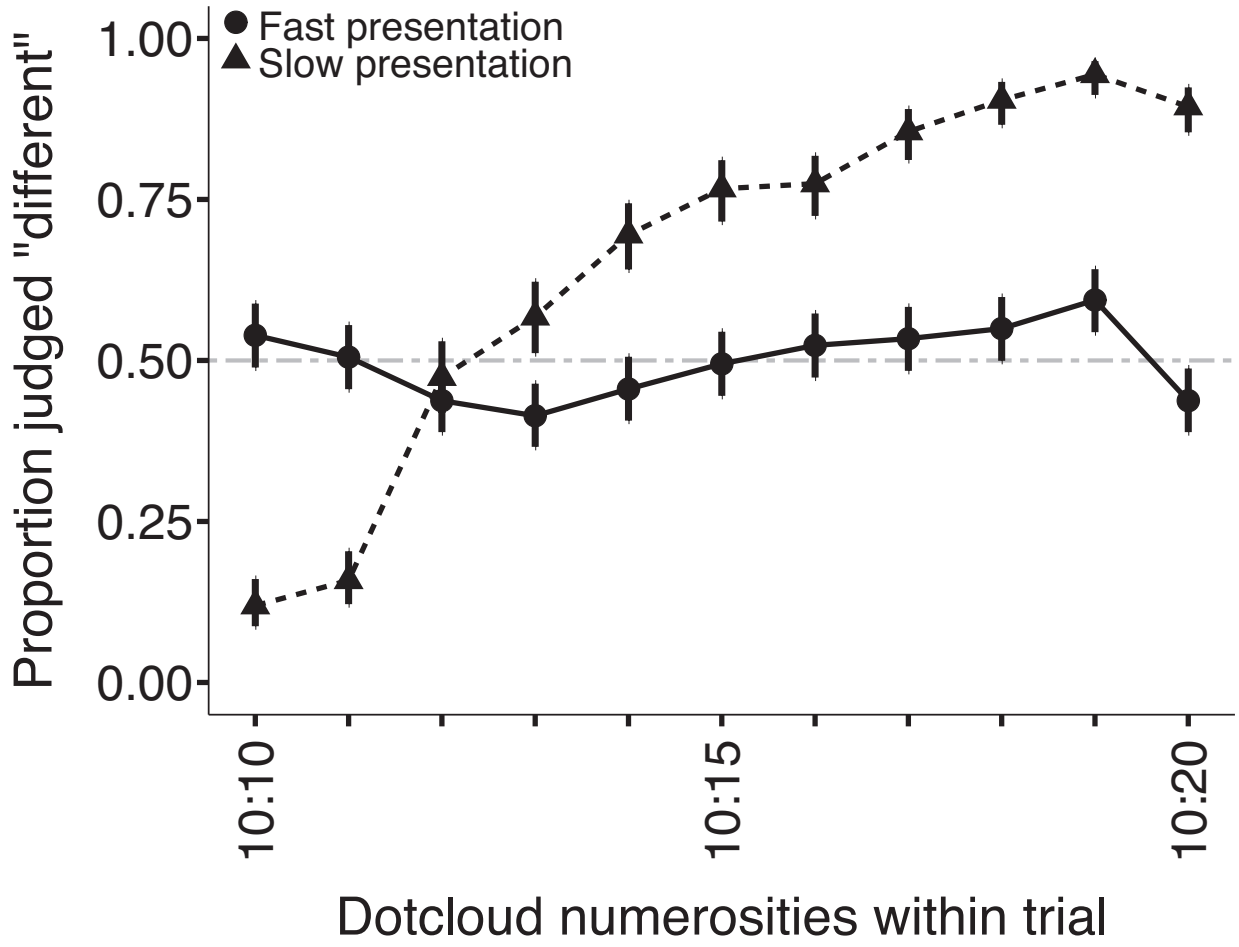

Figure 6. In the task with fast dotcloud presentation, subjects were unable to accurately judge the numerical content of the dotcloud stimuli. When subjects were presented with dotclouds slowly, they were more likely to judge numerosity accurately as the numerical ratio between dotclouds increased. The dotted line shows chance levels of responding. Error bars denote 95% confidence intervals.

Discussion

When subjects viewed dotclouds that alternated in numerosity at 15 Hz, this stimulation evoked a steady-state 15 Hz signal (SSVEP) centered over posterior midline electrodes. The strength of the 15 Hz SSVEP depended on the numerical content of the stimuli even when the size and spacing of the dots were controlled, indicating that the SSVEP was generated in part by

processing of numerical information, and not only the spatial attributes of the stimuli. Due to the rapid presentation of stimuli (33 ms between presentation onsets), each dotcloud was backward-masked by the subsequent dotcloud. Accordingly, although the SSVEPs showed sensitivity to the numerosity of the dotclouds, subjects were unable to report the numerical content of the stimuli consciously, indicating that reentrant feedback related to the numerosity of the stimuli from higher-level cortices back to visual cortex was disrupted. These results suggest that approximate number representations arise within visual cortex, rapidly and unconsciously, independent of reentrant feedback from higher cortical regions typically associated with number processing. These findings are consistent with the proposal that numerosity is processed as a "primary visual property" of stimuli, "like color or motion" (Burr and Ross 2008, pg. 1).

Previous neuroimaging experiments have also shown number-sensitive activity in the visual system (Cavdaroglu and Knops 2019; Fornaciai and Park 2018; Park et al. 2015; Park 2018; DeWind et al. 2018). What has remained unclear, however, is whether this number-sensitive activity in the visual system arises from computations within the occipital cortex itself. Under an alternative account, number representations could arise first in the intraparietal sulcus, a cortical region long believed to be where number representations originate (Dehaene et al. 1999; Nieder 2016; Nieder and Miller 2004; Pinel et al. 2001; Zorzi et al. 2002), and the intraparietal sulcus could subsequently feed number representations back to the occipital cortex. If so, the number-sensitive activity in occipital cortex shown in previous experiments would not necessarily provide evidence that occipital cortex *computes* number (e.g., the way it computes color or motion), as opposed to *reflecting* number representations that originated elsewhere. The present results challenge this skeptical account, supporting the view that approximate number representations arise in the occipital cortex.

If the occipital cortex, itself, computes numerosity, does this finding challenge the belief that number is represented in the intraparietal sulcus? Not necessarily. These findings do raise questions, however, about the role intraparietal sulcus plays in number processing. When researchers claim that the intraparietal sulcus computes number on the basis of visual stimuli (e.g., dotclouds), they may implicitly assume that the information fed forward from visual cortex does not include numerical content, but rather includes the visuo-spatial "ingredients" on the basis of which numerosity is computed. The present results suggest that instead (or in addition), visual cortex may send approximate number representations, per se, to the intraparietal sulcus. If so, rather than creating number representations de novo, the intraparietal sulcus may play other roles in numerical cognition, such as making number available for conscious processing (Dehaene et al. 2006) or guiding actions based on number representations (Fischer 2003, Andres et al. 2004, Lasne et al. 2019).

Although the intraparietal sulcus has been identified as the site of amodal number representations (Naccache and Dehaene 2001), it may not contain modality-independent number representations, at all (Bulthé et al. 2014; Cavdaroglu et al. 2015). Rather, the present data are consistent with the possibility that the intraparietal sulcus is important for comparing modality-specific number representations within and between sensory modalities (Cavdaroglu et al. 2015; Nieder 2012).

Additional studies are needed to clarify the relative contributions of the occipital cortex and the intraparietal sulcus to number processing. The rapid SSVEP technique we used here is not well-suited to answer questions about the intraparietal sulcus, given that (a) SSVEPs have been localized primarily to occipital cortex (Andersen et al. 2008; Di Russo et al. 2007; Fawcett et al. 2004; Hillyard et al. 1997; Müller et al. 1997; Sammer et al. 2005), and (b) even if SSVEPs

can be detected beyond occipital cortex, backward masking may disrupt the flow of information between the occipital cortex and the intraparietal sulcus in ways that could alter the way number is typically represented in the intraparietal sulcus (Lamme et al. 2002).

In addition to backward masking, there is another way that rapid presentation of stimuli could disrupt typical intraparietal sulcus processing of stimulus numerosity. Visual features are subject to "temporal resolution" processing constraints; a stimulus can be presented so briefly that particular visual features are not processed and made available for conscious perception. Higher-order cortical areas tend to require more processing time (Holcombe 2009). Our results are agnostic about whether fast presentation of stimuli prevented accurate judgment of numerosity by disrupting reentrant feedback or by exceeding the temporal resolution of higher-order processing. Either kind of disruption would be sufficient to license the main inference we draw from the present data: that the occipital cortex, per se, responds to the numerosity of the stimuli.

The method we have used here may offer a way to unify the study of approximate number across disparate populations. Researchers have created a large variety of approximate number paradigms. Different tests have been developed for adults in different cultures, children, infants, and for different non-human species (e.g., cotton-top tamarins (Hauser et al. 2003; guppies (Agrillo et al. 2012)). Using different tests for different populations complicates any direct comparisons. It may be difficult to make meaningful comparisons between, for example, female mosquitofish choosing a group to join while fleeing a sexually-aggressive male (Agrillo et al. 2007), infants matching beeps to shapes (Izard et al. 2009), and adults choosing between yellow or blue dots (Libertus et al. 2012). Yet, because EEG has been measured in humans of all ages, from week-old infants (Norcia and Tyler 1985) to adults, and also in multiple vertebrate

species from dogs (Kujala et al. 2013) to zebrafish (Hong et al. 2016), it may be possible to adapt the present paradigm for use across diverse samples. In pilot testing, we have found similar SSVEP results to those presented here when adult subjects were not instructed to attend to number and made no behavioral responses, suggesting that this task may be suitable for use with infants and non-human animals. Within-task comparisons across the lifespan and between species could yield insights into how number capacities change during development, and how they have emerged over evolutionary time.

Funding

This research was supported in part by a grant from the James S. McDonnell Foundation (220020236) awarded to Daniel Casasanto and by a grant from the John Templeton Foundation awarded to Daniel Casasanto, Susan Goldin-Meadow, and Edward K. Vogel. This work was presented as a poster at the 25th annual meeting of the Cognitive Neuroscience Society in Boston, MA.

Notes

Correspondence concerning this article should be addressed to Daniel Casasanto, Department of Human Development, Cornell University, Ithaca, NY 14853. Contact: casasanto@alum.mit.edu

Conflict of Interest: The authors declare no conflicting interests.

References

Agrillo C, Dadda M, Bisazza A. 2007. Quantity discrimination in female mosquitofish. *Anim Cogn*. 10:63-70.

Agrillo C, Piffer L, Bisazza A, Butterworth B. 2012. Evidence for two numerical systems that are similar in humans and guppies. *PLoS One*. 7: e31923.

Andres M, Pelgrims B, Michaux N, Olivier E, Pesenti M. 2011. Role of distinct parietal areas in arithmetic: an fMRI-guided TMS study. *NeuroImage*. 54:3048-3056.

Andres M, Davare M, Pesenti M, Olivier E, Seron X. 2004. Number magnitude and grip aperture interaction. *Neuroreport*. 15:2773-2777.

Andersen SK, Hillyard SA, Müller MM. 2008. Attention facilitates multiple stimulus features in parallel in human visual cortex. *Curr Biol.* 18:1006-1009.

Arrighi R, Togoli I, Burr DC. 2014. A generalized sense of number. *Proc R Soc Lond B Biol Sci.* 281:20141791.

Barr DJ, Levy R, Scheepers C, Tily HJ. 2013. Random effects structure for confirmatory hypothesis testing: Keep it maximal. *J Mem Lang.* 68:255-278.

Bates D, Mächler M, Bolker B, Walker S. 2015. Fitting linear mixed-effects models using lme4. J Stat Softw. 67:1-48.

Bulthé J, De Smedt B, Op de Beeck H. 2014. Format-dependent representations of symbolic and non-symbolic numbers in the human cortex as revealed by multi-voxel pattern analyses. *NeuroImage.* 87:311-322.

Burr D, Ross J. 2008. A visual sense of number. *Curr Biol.* 18:425-428.

Cappelletti M, Barth H, Fregni F, Spelke ES, Pascual-Leone A. 2007. rTMS over the intraparietal sulcus disrupts numerosity processing. *Experimental Brain Res.* 179:631.

Castaldi E, Piazza M, Dehaene S, Vignaud A, Eger E. 2019. Attentional amplification of neural codes for number independent of other quantities along the dorsal visual stream. *Elife.* 8*:e45160.*

Cavdaroglu S, Katz C, Knops A. 2015. Dissociating estimation from comparison and response eliminates parietal involvement in sequential numerosity perception. *NeuroImage.* 116:135-148.

Cavdaroglu S, Knops A. 2019. Evidence for a posterior parietal cortex contribution to spatial but not temporal numerosity perception. *Cereb Cortex.* 29:2965-2977.

Cipolotti L, Butterworth B, Denes G. 1991. A specific deficit for numbers in a case of dense acalculia. *Brain*. 114:2619-2637.

Di Lollo V, Enns JT, Rensink RA. 2000. Competition for consciousness among visual events: the psychophysics of reentrant visual processes. *J Exp Psychol Gen.* 129:481-507.

Dehaene S, Changeux JP, Naccache L, Sackur J, Sergent C. 2006. Conscious, preconscious, and subliminal processing: a testable taxonomy. *Trends Cogn Sci*. 10:204-211.

Dehaene S, Cohen L. 1997. Cerebral pathways for calculation: Double dissociation between rote verbal and quantitative knowledge of arithmetic. *Cortex*. 33:219-250.

Dehaene S, Dehaene-Lambertz G, Cohen L. 1998. Abstract representations of numbers in the animal and human brain. *Trends Neurosci*. 21:355-361.

Dehaene S, Piazza M, Pinel P, Cohen L. 2003. Three parietal circuits for number processing. *Cogn Neuropsychol.* 20:487-506.

Dehaene S, Spelke E, Pinel P, Stanescu R, Tsivkin S. 1999. Sources of mathematical thinking: Behavioral and brain-imaging evidence. *Science*. 284:970-974.

DeWind NK, Adams GK, Platt ML, Brannon EM. 2015. Modeling the approximate number system to quantify the contribution of visual stimulus features. *Cognition*. 142:247-265.

DeWind NK, Park J, Woldorff MG, Brannon EM. 2018. Numerical encoding in early visual cortex. *Cortex*. 114:76-89.

Di Russo F, Pitzalis S, Aprile T, Spitoni G, Patria F, Stella A, Spinelli D, Hillyard SA. 2007. Spatiotemporal analysis of the cortical sources of the steady-state visual evoked potential. *Hum Brain Mapp.* 28:323-334.

Dumoulin SO, Dakin SC, Hess RF. 2008. Sparsely distributed contours dominate extra-striate responses to complex scenes. *NeuroImage*. 42:890-901.

Dux PE, Visser TA, Goodhew SC, Lipp OV. 2010. Delayed reentrant processing impairs visual awareness: An object-substitution-masking study. *Psychol Sci.* 21:1242-1247.

Eger E, Sterzer P, Russ MO, Giraud AL, Kleinschmidt A. 2003. A supramodal number representation in human intraparietal cortex. *Neuron*. 37:719-726.

Fawcett IP, Barnes GR, Hillebrand A, Singh KD. 2004. The temporal frequency tuning of human visual cortex investigated using synthetic aperture magnetometry. *NeuroImage*. *21*:1542-1553.

Fischer M. 2003. Spatial representations in number processing--evidence from a pointing task. *Vis Cogn*. 10:493-508.

Fornaciai M, Brannon EM, Woldorff MG, Park J. 2017. Numerosity processing in early visual cortex. *NeuroImage*. 157:429-438.

Fornaciai M, Park J. 2018. Neural Sensitivity to Numerosity in Early Visual Cortex Is Not Sufficient for the Representation of Numerical Magnitude. *J Cogn Neurosci*. 30:1788-1802.

Fahrenfort JJ, Scholte HS, Lamme VA. 2007. Masking disrupts reentrant processing in human visual cortex. *J Cogn Neurosci.* 19:1488-1497.

Göbel SM, Rushworth MF, Walsh V. 2006. Inferior parietal rTMS affects performance in an addition task. *Cortex*. 42:774-781.

Hauser MD, Tsao F, Garcia P, Spelke ES. 2003. Evolutionary foundations of number: spontaneous representation of numerical magnitudes by cotton top tamarins. *Proc R Soc Lond B Biol Sci.* 270:1441-1446.

Hillyard SA, Hinrichs H, Tempelmann C, Morgan ST, Hansen JC, Scheich H, Heinze HJ. 1997. Combining steady-state visual evoked potentials and fMRI to localize brain activity during selective attention. *Hum Brain Mapp.* 5:287-292.

Holcombe AO. 2009. Seeing slow and seeing fast: two limits on perception. *Trends Cogn Sci.* 13:216-221.

Hong S, Lee P, Baraban SC, Lee LP. 2016. A novel long-term, multi-channel and non-invasive electrophysiology platform for zebrafish. *Sci Rep*. 6:28248.

Izard V, Sann C, Spelke ES, Streri, A. 2009. Newborn infants perceive abstract numbers. *Proc Natl Acad Sci*. 106:10382-10385.

Kujala MV, Törnqvist H, Somppi S, Hänninen L, Krause CM, Vainio O, Kujala J. 2013. Reactivity of dogs' brain oscillations to visual stimuli measured with non-invasive electroencephalography. *PLoS One*. 8:e61818.

Kukkonen H, Rovamo J, Tiippana K, Näsänen R. 1993. Michelson contrast, RMS contrast and energy of various spatial stimuli at threshold. *Vision Res*. 33:1431-1436.

Lamme VA. 2003. Why visual attention and awareness are different. *Trends Cogn Sci*. 7:12-18.

Lamme VA. 2006. Towards a true neural stance on consciousness. *Trends Cogn Sci*. 10:494-501.

Lamme VA, Roelfsema PR. 2000. The distinct modes of vision offered by feedforward and recurrent processing. *Trends Neurosci*. 23:571-579.

Lamme VA, Zipser K, Spekreijse H. 2002. Masking interrupts figure-ground signals in V1. *J Cogn Neurosci*. 14:1044-1053.

Lasne G, Piazza M, Dehaene S, Kleinschmidt A, Eger E. 2019. Discriminability of numerosity-evoked fMRI activity patterns in human intra-parietal cortex reflects behavioral numerical acuity. *Cortex.* 114:90-101.

Libertus ME, Brannon EM, Woldorff MG. 2011. Parallels in stimulus-driven oscillatory brain responses to numerosity changes in adults and seven-month-old infants. *Dev Neuropsychol*. 36:651-667.

Libertus ME, Odic D, Halberda J. 2012. Intuitive sense of number correlates with math scores on college-entrance examination. *Acta Psychologica.* 141:373-379.

Naccache L, Dehaene S. 2001. The priming method: imaging unconscious repetition priming reveals an abstract representation of number in the parietal lobes. *Cereb Cortex*. 11:966-974.

Nieder A. 2012. Supramodal numerosity selectivity of neurons in primate prefrontal and posterior parietal cortices. *Proc Natl Acad Sci.* 109:11860-11865.

Nieder A. 2016. The neuronal code for number. *Nat Rev Neurosci.* 17:366-382.

Nieder A, Miller EK. 2004. A parieto-frontal network for visual numerical information in the monkey. *Proc Natl Acad Sci.* 101:7457-7462.

Norcia AM, Appelbaum LG, Ales JM, Cottereau BR, Rossion B. 2015. The steady-state visual evoked potential in vision research: a review. *J Vis*. 15:4-4.

Norcia AM, Tyler CW. 1985. Spatial frequency sweep VEP: visual acuity during the first year of life. *Vision Res*. 25:1399-1408.

Oostenveld R, Fries P, Maris E, Schoffelen JM. 2011. FieldTrip: open source software for advanced analysis of MEG, EEG, and invasive electrophysiological data. *Comput Intell Neurosci*. 2011:156869.

Oram MW, Perrett DI. 1992. Time course of neural responses discriminating different views of the face and head. *J Neurophysiol*. 68:70-84.

Parish DH, Sperling G. 1991. Object spatial frequencies, retinal spatial frequencies, noise, and the efficiency of letter discrimination. *Vision Res*. 31:1399-1415.

Park J. 2018. A neural basis for the visual sense of number and its development: A steady-state visual evoked potential study in children and adults. *Dev Cogn Neurosci*. 30:333-343.

Park J, DeWind NK, Woldorff MG, Brannon EM. 2015. Rapid and direct encoding of numerosity in the visual stream. *Cereb Cortex*. 26:748-763.

Peirce JW. 2007. PsychoPy—psychophysics software in Python. *J Neurosci Methods*. 162:8-13.

Piazza M, Pinel P, LeBihan, D, Dehaene S. 2007. A magnitude code common to numerosities and number symbols in human intraparietal cortex. *Neuron*. 53:293-305.

Pinel P, Dehaene S, Rivière D, LeBihan D. 2001. Modulation of parietal activation by semantic distance in a number comparison task. *NeuroImage*. 14:1013-1026.

R Core Team. 2016. R: a language and environment for statistical computing. R Foundation for Statistical Computing.

Rossion B, Prieto EA, Boremanse A, Kuefner D, Van Belle G. 2012. A steady-state visual evoked potential approach to individual face perception: effect of inversion, contrast-reversal and temporal dynamics. *NeuroImage*. 63:1585-1600.

Sammer G, Blecker C, Gebhardt H, Kirsch P, Stark R, Vaitl D. 2005. Acquisition of typical EEG waveforms during fMRI: SSVEP, LRP, and frontal theta. *NeuroImage*. 24:1012-1024.

Srinivasan R, Russell DP, Edelman GM, Tononi G. 1999. Increased synchronization of neuromagnetic responses during conscious perception. *J Neurosci*. 19:5435-5448.

Zorzi M, Priftis K, Umiltà C. 2002. Brain damage: neglect disrupts the mental number line. *Nature*. 417:138-139.

Supplementary Materials

Trial videos

Here we provide links to videos showing trials with "fast" and "slow" dotcloud presentation. Subjects showed little ability to report on the numerosity of dotclouds during the fast stimulation task (Fig. 6). In contrast, subjects were able to accurately judge the numerical content of the dotcloud stimuli during slow presentation.

The fast dotcloud presentation video has a flashing patch in the bottom left corner. A photodiode covered the patch during testing.

10 : 14 trial, fast presentation.mov
10 : 14 trial, slow presentation.mov

Variance explained by non-numeric attributes with and without controlling for number

In Table 1 we report the variance explained by each of the attributes individually, and while controlling for the effect of dotcloud numerosity.

We used the *MuMIn* package in R to calculate the R^2 values. The R^2 value is the result of comparing the loglikelihoods of a full model and a reduced model. We include random subject slopes for the attribute of interest and random subject intercepts when calculating full models as explained in *Materials and Methods*. The reduced models drop both the fixed effect for the attribute of interest, and the random subject slopes for that attribute so that the null model contained no information about that attribute.

All models were significant at $p < .001$, indicating that the non-numerical attributes of the stimuli contribute to the SSVEP as well.

Table 1.

Attribute	R^2	R^2 controlling for Number
Number	.1559	-
Total Surface Area	.1058	.0079
Individual Dot Size	.0816	.0672
Convex Hull	.1273	.0595
Sparsity	.0239	.0511
Size	.0550	.0623
Spacing	.0288	.0483
Contrast Energy	.1004	.0028

Description of dotcloud stimuli

Table 2 contains the ranges of the non-numerical stimuli attributes within each of the 11 trials.

Table 2.

Num	TSA	IDS	CH	Sparsity (1/density)	Sz	Sp	CE
10 : 10	7080 : 7080	708 : 708	155294 : 216097	15529 : 21609	5012640 : 5012640	2411560526 : 4669640073	867 : 867
10 : 11	8932 : 9040	812 : 904	231185 : 337692	23118 : 30699	7252784 : 8172160	5344534830 : 10366806708	1091 : 1104
10 : 12	23520 : 24560	1960 : 2456	116889 : 231838	11688 : 19319	46099200 : 60319360	1366198632 : 4478878322	2818 : 2939
10 : 13	43163 : 47520	3608 : 4752	106862 : 247066	10686 : 19005	169229632 : 225815040	1141927332 : 4695489330	5038 : 5515
10 : 14	52292 : 57760	4052 : 5776	124439 : 296745	12443 : 21196	229861856 : 333621760	1548394477 : 6289807020	6030 : 6612
10 : 15	65623 : 72000	4752 : 7200	150622 : 365747	15062 : 24383	338722560 : 518400000	2268668564 : 8918009101	7433 : 8086
10 : 16	65278 : 72128	4508 : 7200	150483 : 365711	15048 : 22856	325153024 : 518400000	2264468184 : 8358690616	7397 : 8099
10 : 17	34745 : 41752	2456 : 3836	85348 : 265653	8534 : 15626	102542912 : 147148960	728359832 : 4151093778	4102 : 4883
10 : 18	22281 : 27360	1520 : 2456	69053 : 241029	6905 : 13390	41587200 : 60319360	476810965 : 3227378310	2674 : 3262
10 : 19	15114 : 19380	1020 : 1664	53103 : 215969	5310 : 11366	19767600 : 27688960	281976930 : 2454703654	1831 : 2335
10 : 20	9360 : 12160	608 : 1020	33373 : 165130	3337 : 8256	7393280 : 10404000	111365701 : 1363313280	1143 : 1479

Coherent (phase-aware) SNR plots

Fourier results can be combined by scalar or vector averaging. Scalar averaging uses only the magnitude and discards the phase information. Vector-averaging makes use of both the magnitude and the phase information; the complex Fourier components are projected onto the complex plane, and then the x and y values of each component are averaged separately. Assuming the phase of the noise is randomly distributed and that the phase of the signal is consistent across trials, the expected value of the noise's contribution to the signal's magnitude is 0, so the SNR increases with additional data. The vector-based method yields a more accurate estimate of the *average* signal (reflected by a higher SNR) at the cost of discarding information about trial-level signal variation. Here we adapt Fig. 4 and Fig. 5 from the main text using vector averaging to calculate the SNR. We excluded one subject's data from the SNR calculations because their photodiode data was missing and so we could not phase-lock their trials.

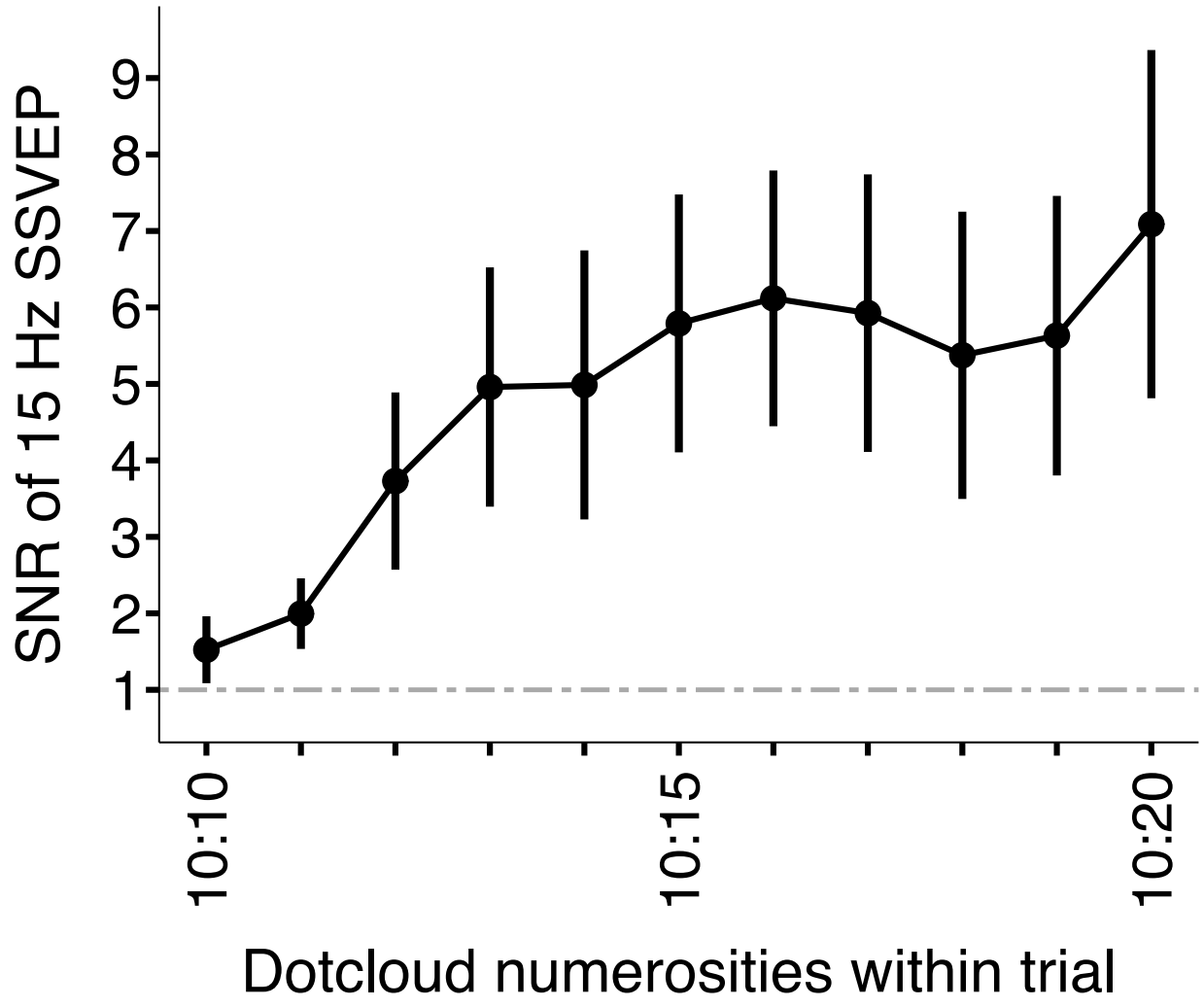

Figure 7. The signal-to-noise ratio of the 15 Hz SSVEP calculated with vector averaging. The dashed line indicates a signal-to-noise ratio of 1. Error bars denote 95% confidence intervals.

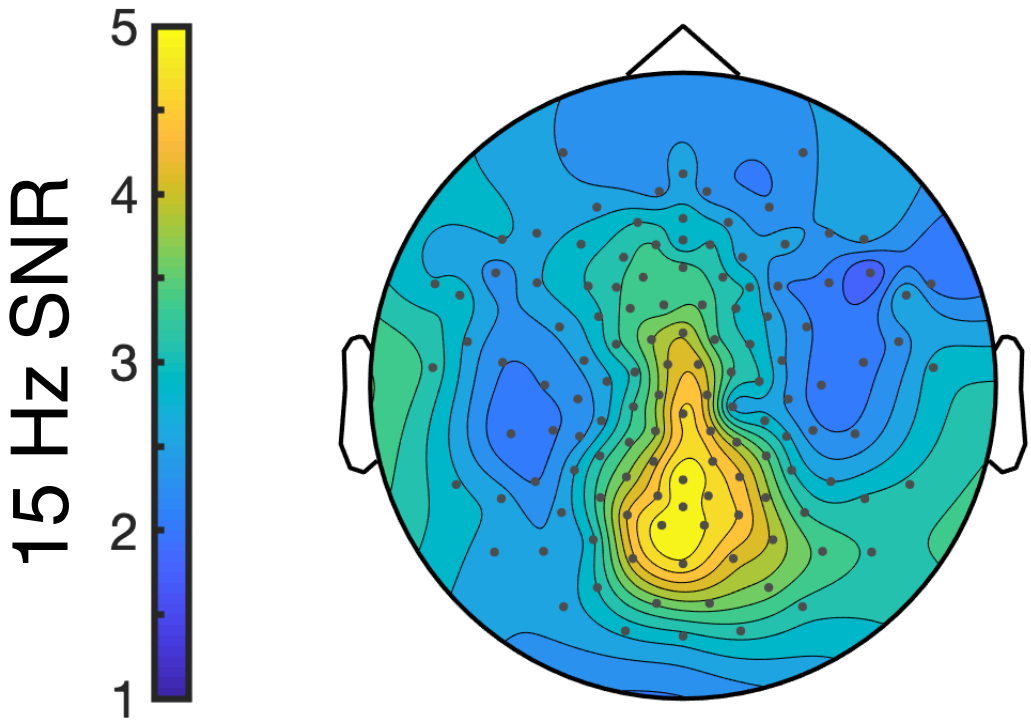

Figure 8. Grand averaged 15 Hz SSVEP SNR calculated using vector averaging.